Proc. Natl. Acad. Sci. USA
Vol. 92, pp. 5149–5153, May 1995
Biochemistry

Definition of a metal-dependent/Li^+-inhibited phosphomonoesterase protein family based upon a conserved three-dimensional core structure

(inositol, fructose, and 3-phosphoadenosine 5'-phosphosulfate phosphatases/evolution/metal-binding motif/manic depressive disease)

JOHN D. YORK*†, JAY W. PONDER‡, AND PHILIP W. MAJERUS*‡

*Division of Hematology–Oncology, and ‡Department of Biochemistry and Molecular Biophysics, Washington University School of Medicine, Box 8125, 660 South Euclid Avenue, St. Louis, MO 63110

Contributed by Philip W. Majerus, February 21, 1995

ABSTRACT **Inositol polyphosphate 1-phosphatase, inositol monophosphate phosphatase, and fructose 1,6-bisphosphatase share a sequence motif, Asp-Pro-(Ile or Leu)-Asp-(Gly or Ser)-(Thr or Ser), that has been shown by crystallographic and mutagenesis studies to bind metal ions and participate in catalysis. We compared the six α-carbon coordinates of this motif from the crystal structures of these three phosphatases and found that they are superimposable with rms deviations ranging from 0.27 to 0.60 Å. Remarkably, when these proteins were aligned by this motif a common core structure emerged, defined by five α-helices and 11 β-strands comprising 155 residues having rms deviations ranging from 1.48 to 2.66 Å. We used the superimposed structures to align the sequences within the common core, and a distant relationship was observed suggesting a common ancestor. The common core was used to align the sequences of several other proteins that share significant similarity to inositol monophosphate phosphatase, including proteins encoded by fungal *qa-X* and *qutG*, bacterial *suhB* and *cysQ* (identical to *amtA*), and yeast *met22* (identical to *hal2*). Evolutionary comparison of the core sequences indicate that five distinct branches exist within this family. These proteins share metal-dependent/Li^+-sensitive phosphomonoesterase activity, and each predicted tree branch exhibits unique substrate specificity. Thus, these proteins define an ancient structurally conserved family involved in diverse metabolic pathways including inositol signaling, gluconeogenesis, sulfate assimilation, and possibly quinone metabolism. Furthermore, we suggest that this protein family identifies candidate enzymes to account for both the therapeutic and toxic actions of Li^+ as it is used in patients treated for manic depressive disease.**

Inositol polyphosphate 1-phosphatase (1-ptase) and inositol monophosphate phosphatase (m-ptase) are two critical enzymes in the inositol signaling pathway that share similar enzymatic properties (1–3). Both enzymes exhibit an absolute requirement for metal ions (Mg^{2+} is preferred), and both are uncompetitively inhibited by submillimolar concentrations of Li^+. 1-ptase catalyzes the removal of the 1-phosphate from inositol 1,4-bisphosphate or inositol 1,3,4-trisphosphate to form inositol 4-phosphate or inositol 3,4-bisphosphate. m-ptase removes equatorially positioned phosphates from inositol monophosphates to yield inositol. Interestingly, despite having similar catalytic properties and substrates, the sequences of 1-ptase and m-ptase do not exhibit any obvious similarity, except for a short sequence motif, Asp-Pro-Ile-Asp-(Gly or Ser)-Thr (4). This motif was later found to be conserved in several other proteins related to m-ptase including products of fungal *qa-X* and *qutG*, bacterial *suhB* and *cysQ* (identical to *amtA*), and yeast *met22* (identical to *hal2*) (5, 6). The conservation of this sequence suggested that it might play an important functional role. This has been confirmed by the recent determination of the crystal structures of 1-ptase and m-ptase solved in the presence of metal ions (7, 8). In both proteins, residues in this motif participate in metal binding and are located near the catalytic site. Despite lacking an apparent evolutionary relationship, the structures of both proteins share similar α/β/α/β folds (7, 8). Recently, Zhang *et al.* (9) noted that the fold of fructose 1,6-bisphosphatase (fb-ptase) is identical to that of m-ptase. fb-ptase is a critical allosterically regulated enzyme in the gluconeogenic pathway that removes the 1-phosphate from fructose 1,6-bisphosphate to form fructose 6-phosphate (10, 11). fb-ptase also requires metal ions for catalysis, Mg^{2+} and Mn^{2+} are preferred, and fb-ptase is potently inhibited by Li^+, although the pattern of inhibition has not been described (10–14). fb-ptase has a metal binding sequence, Asp-Pro-Leu-Asp-Gly-Ser, and the structure of fb-ptase solved in the presence of Mg^{2+} demonstrates that this sequence binds metal ions (15).

In the present study, we have assessed the structural relationship of this motif using the x-ray structures of 1-ptase, m-ptase, and fb-ptase. This analysis has led to the identification of a common core structure shared by all three proteins consisting of 155 residues. The common core structure includes the residues essential for metal binding and those needed for catalysis, providing a structural basis for the conserved enzymatic properties of these enzymes. Additionally, we have expanded this family to include several other proteins, and we conclude that these proteins will also have the common core structure and identical metal-dependent/Li^+-sensitive catalytic mechanisms. Comparisons of these conserved structures will facilitate rational design of specific inhibitors aimed at mimicking the actions of Li^+ as potential therapies for patients suffering from manic depressive disease.

METHODS

Least-squares superimposition of the core structures of 1-ptase, m-ptase, and fb-ptase was performed by using INSIGHTII with the α-carbon coordinates obtained from 1inp, 2hhm (A subunit), and 1fbp (A subunit) PDB files in the Brookhaven Protein Data Bank. Sequence motif residues 153–158 of 1-ptase, 90–95 of m-ptase, and 118–123 of fb-ptase were used for initial superimposition. From this alignment a common core structure emerged, including 1-ptase residues 3–23, 52–67, 74–81, 148–158, 159–164, 181–190, 195–205, 217–223, 228–233, 263–268, 283–290, 291–301, 304–308, 312–328, 329–334, and 372–377; m-ptase residues 7–27, 45–60,

The publication costs of this article were defrayed in part by page charge payment. This article must therefore be hereby marked "*advertisement*" in accordance with 18 U.S.C. §1734 solely to indicate this fact.

Abbreviations: 1-ptase, inositol polyphosphate 1-phosphatase; m-ptase, inositol monophosphate phosphatase; fb-ptase, fructose 1,6-bisphosphatase.

†To whom reprint requests should be addressed.

65–72, 85–95, 96–101, 104–113, 116–126, 128–134, 136–141, 157–162, 188–195, 196–206, 209–213, 215–231, 232–237, and 249–254; and fb-ptase residues 28–48, 72–87, 92–99, 113–123, 124–129, 131–140, 158–168, 171–177, 178–183, 207–212, 240–247, 248–258, 260–264, 275–291, 292–297, and 315–320. α-Carbon coordinates for these residues were used for superimpositions of the common core structures.

The alignment of the core sequences of bovine 1-ptase, human m-ptase, and porcine fb-ptase was performed on the basis of equivalent positions in the superimposed common core structure. Sequences encoded by *Neurospora crassa qa-X, Aspergillus nidulans qutG, Escherichia coli suhB, E. coli cysQ* (which is identical to *amtA*), and *Saccharomyces cerevisiae met22* (which is identical *hal2*) were aligned by carrying out searches with the TBLASTN program (16) in which all family members except 1-ptase and fb-ptase were compared pairwise at a cutoff score of 30. This allowed optimal alignment of all core elements except for β_7 for met22 and β_{11} for most of the members. For these elements, alignments were made by using sequence spatial constraints and a manual iterative alignment to maximize similarities. The amino acid similarity at each position in the core structure was determined by using the Dayhoff mutation data matrix (17). The percent maximal score for each residue is defined by summation of mutation scores for each protein when compared to 1-ptase divided by the maximal score—i.e., the score achieved when all residues were identical to 1-ptase. For example, the terminal residue of the core element β1 is serine in 1-ptase and is serine, aspartic acid, or threonine in the other family members. The mutation data matrix scores for serine, aspartic acid, and threonine are 4, 2, and 3, respectively. Thus, the percent maximal score of 84% is equal to the observed score [(4·5) + (2·2) + 3] divided by the maximal score (4·8) multiplied by 100.

The evolutionary tree was constructed by using the PILEUP program of the Genetic Computer Group suite (18) based on a simplification of the progressive alignment method of Feng and Doolittle (19). Core sequence elements as defined above were concatenated to form a continuous sequence and used as input for PILEUP. When multiple species were available, sequences were first aligned by using TBLASTN to identify their core sequences, which were then concatenated and used as input for PILEUP.

RESULTS AND DISCUSSION

We assessed the structural relationship of the Asp-Pro-(Ile or Leu)-Asp-(Gly or Ser)-(Thr or Ser) sequence motif found in 1-ptase, m-ptase, and fb-ptase by superimposition of the six α-carbon coordinates from their x-ray structures. rms deviations of 0.27 Å, 0.54 Å, and 0.60 Å were obtained when comparing

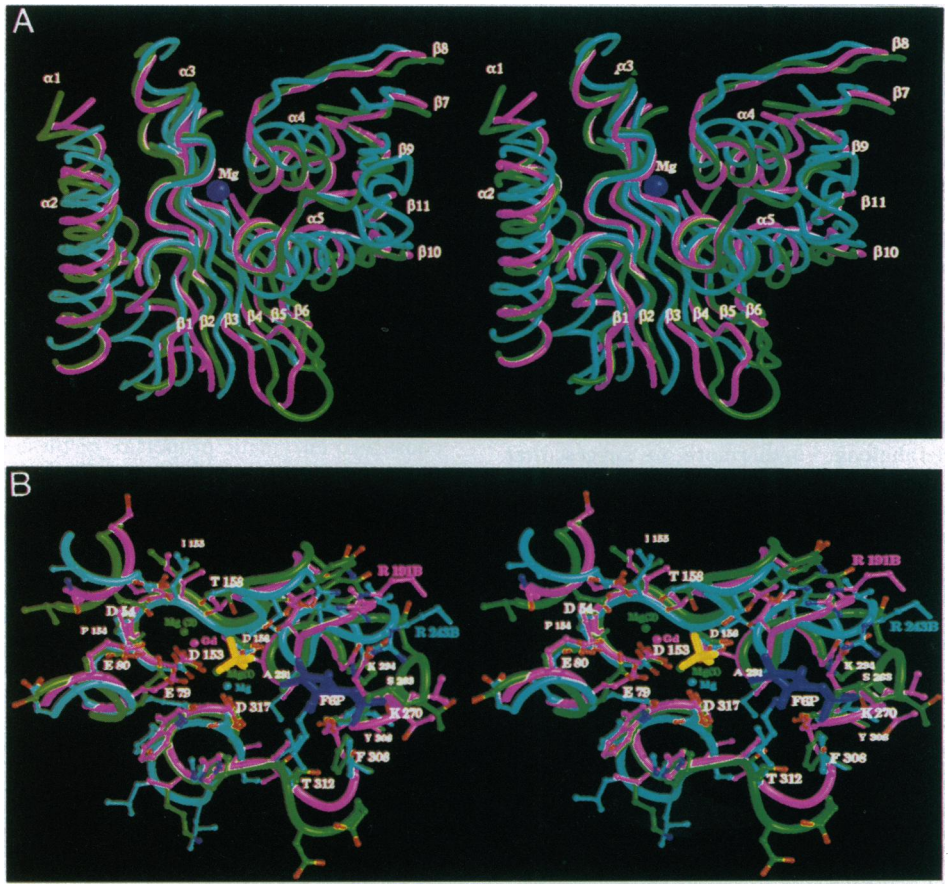

FIG. 1. Stereo image of the superimposed core structures (*A*) and active-site pockets (*B*) of 1-ptase, m-ptase, and fb-ptase. (*A*) Least-squares superimposition of the core structures of 1-ptase, m-ptase, and fb-ptase. The 155 residues included in the core structure superimposition are the same as defined in Fig. 2*A*. rms deviations are 1.48 Å for 1-ptase vs. m-ptase, 2.16 Å for m-ptase vs. fb-ptase, and 2.66 Å for 1-ptase vs. fb-ptase. The core secondary structure elements, α-helices and β-sheets, are numbered sequentially. A single Mg^{2+}, corresponding to the metal site 1 of 1-ptase, is shown as a dark blue sphere. 1-ptase, m-ptase, and fb-ptase are colored green, magenta, and cyan, respectively. (*B*) m-ptase, 1-ptase, and fb-ptase core structures were superimposed, and selected residues within a 12-Å radius of metal site 1 (1-ptase) are shown. White labels correspond to 1-ptase numbering; the magenta and cyan labels correspond to the B-subunit residues from m-ptase and fb-ptase, respectively. Metal ions are colored to match the respective backbones. The m-ptase structure includes a single gadolinium (Gd^{3+}) metal ion and a sulfate ion (yellow). The fb-ptase structure includes a single Mg^{2+} metal ion and fructose 6-phosphate (dark blue). Side-chain oxygens involved in metal coordination are colored red. Water molecules are omitted for clarity. Both figures were stylized by using MIDAS.

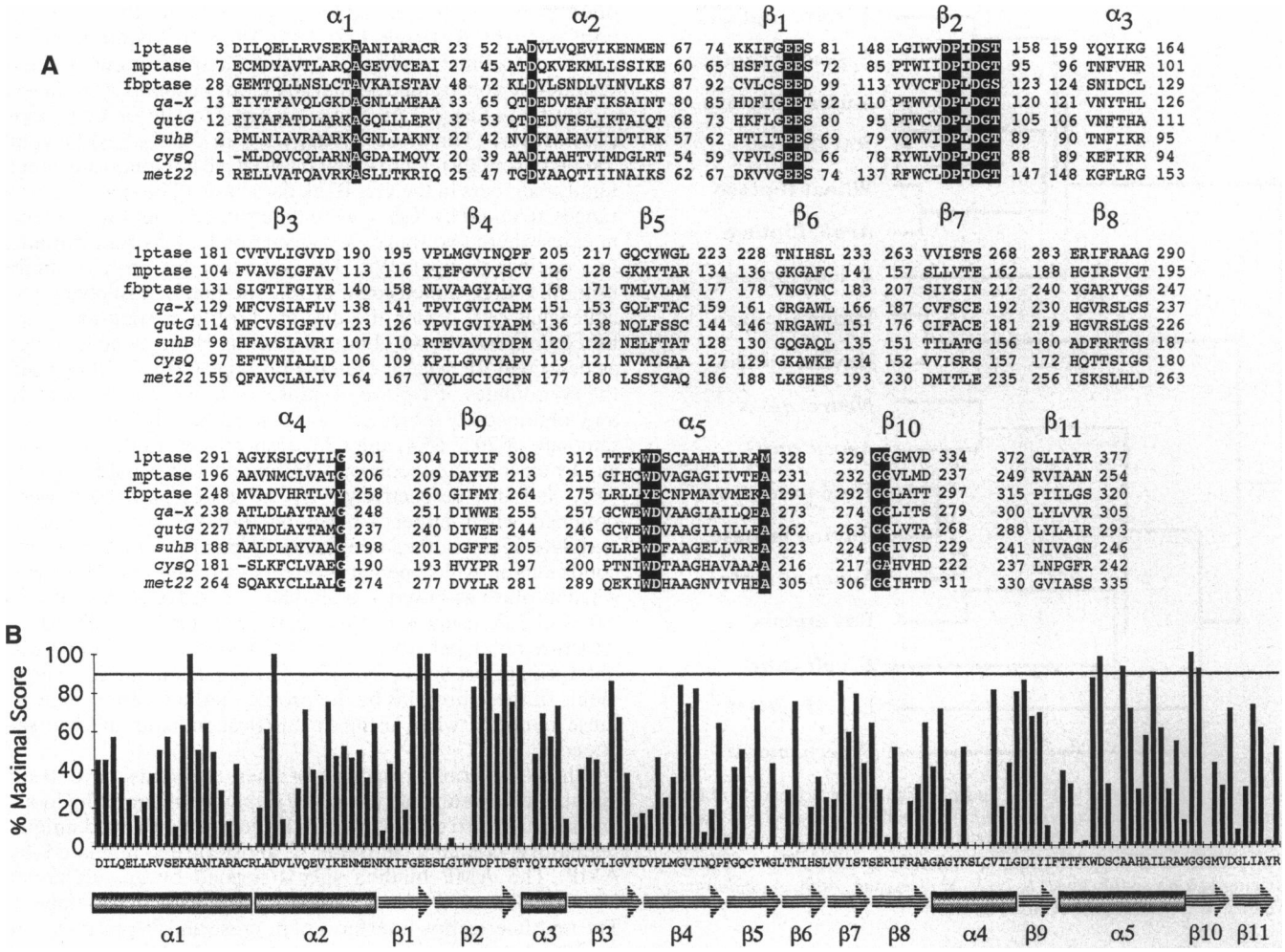

FIG. 2. Alignment and similarity of the common core sequences of a putative family of metal-dependent/Li^+-sensitive phosphomonoesterases. (*A*) The alignment of the core sequences of bovine 1-ptase, human m-ptase, and porcine fb-ptase based upon equivalent positions in the superimposed common core structure. Sequences of *N. crassa* Qa-X, *A. nidulans* QutG, *E. coli* SuhB, *E. coli* CysQ, and *S. cerevisiae* met22 were aligned as described in text. Positions in which >87% sequence identity is observed are highlighted. Residue numbers for each protein flank each core element. (*B*) The amino acid similarity at each position in the core structure as determined with the Dayhoff mutation data matrix. The percent maximal score for each residue is defined by summation of mutation scores for each protein when compared with 1-ptase divided by the maximal score. Each core secondary structure element is diagramed below sequences and correspond to those defined in Fig. 1*A*.

1-ptase vs. fb-ptase, fb-ptase vs. m-ptase, and 1-ptase vs. m-ptase, respectively. When this motif was aligned, a common core structure emerged as defined by five α-helices and 11 β-sheets comprising 155 residues out of a total of 400 (1-ptase), 278 (m-ptase), and 338 (fb-ptase). Superimposition of these 155 α-carbon coordinates is shown in Fig. 1*A* with rms deviations of 1.48 Å for 1-ptase vs. m-ptase, 2.16 for m-ptase vs. fb-ptase, and 2.66 for 1-ptase vs. fb-ptase.

Despite sharing a highly conserved core structure and similar catalytic properties, 1-ptase, m-ptase, and fb-ptase exhibit no overlap in substrate specificity. Therefore, we compared the active-site pockets of the superimposed 1-ptase, m-ptase, and fb-ptase structures as shown in Fig. 1*B*. The metal binding residues (1-ptase numbering) Asp-54, Glu-79, Glu-80, Asp-153, Ile-155, Asp-156, and Asp-317 are highly conserved among the three proteins in both sequence and three-dimensional position. Another conserved residue, Thr-158, does not bind metal based on the crystal structure of the 1-ptase–Mg^{2+} complex (7) but has been shown to be absolutely required for catalysis (20, 21). The x-ray structures of the fb-ptase–product and m-ptase–substrate have been determined (15, 22). Residues involved in specific substrate or product interactions are not conserved among 1-ptase, m-ptase, and fb-ptase. Distinct differences in the backbone positions are also observed in some regions of the substrate binding pockets, thereby constraining the active sites. In addition, multimerization of m-ptase and fb-ptase results in introduction of an arginine residue into the substrate binding region (m-ptase, position 191 of the B subunit; fb-ptase, position 243 of the B subunit). In contrast, in the 1-ptase structure, all of the substrate binding and catalytic residues are contained within the monomer. The common core structure and unique substrate specificities of these proteins make them an ideal family for detailed crystallographic and mutagenesis studies aimed at understanding the origins of enzyme diversity, similar to the triose isomerase (TIM)-barrel fold protein family as reviewed by Petsko and colleagues (23).

Our previous attempts to show sequence similarity of 1-ptase, m-ptase, or fb-ptase using TBLASTN sequence alignment have failed. Therefore, we used the superimposed structures to align the common core sequence elements of 1-ptase, m-ptase, and fb-ptase as shown in Fig. 2*A*. Visual comparison of the core sequences of these three proteins shows that they are indeed related. We then aligned the sequences of several proteins including fungal Qa-X and QutG, bacterial SuhB and CysQ, and yeast met22, for which the crystal structures are not known (6, 24–28). These proteins share the Asp-Pro-(Ile or Leu)-Asp-(Gly or Ser)-(Thr or Ser) metal-binding motif and

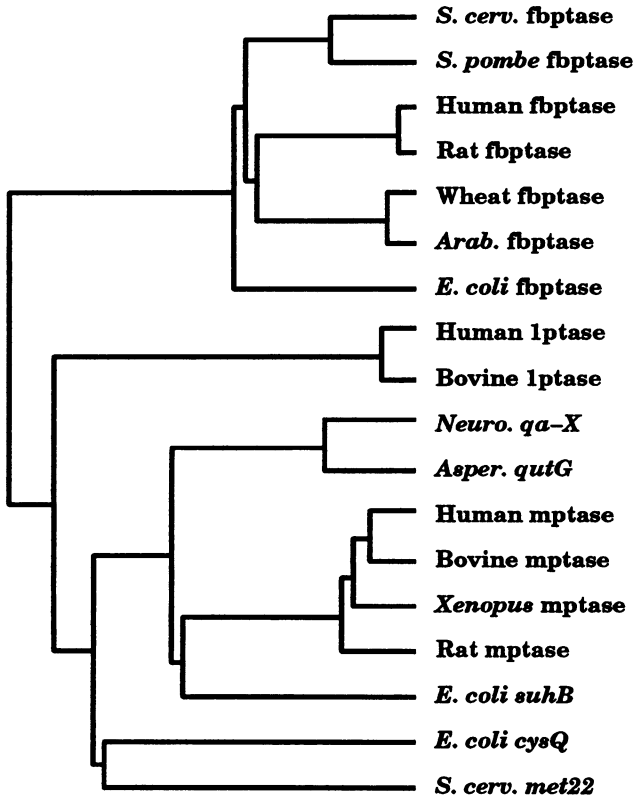

FIG. 3. Evolutionary tree of the putative metal-dependent/Li^+-sensitive phosphomonoesterases family members. The tree was constructed using the PILEUP program. The horizontal distances indicate the degree of divergence from a common ancestor. The vertical spacing has no significance. *S. cerv., S. cerevisiae; Arab, Arabidopsis; Neuro., N. crassa; Asper., A. nidullans.*

have significant overall sequence similarity with m-ptase (5, 6). The similarity of these eight proteins at each position in the core structure was assessed by using the Dayhoff mutation data matrix as shown in Fig. 2*B*. Sixty-five residues have scores >50% of the maximal score. Strikingly, there are 12 residues scattered throughout the core structure that are highly conserved (>90% maximal score) as highlighted in Fig. 2*B*. Six of these residues coordinate metal ions, and one does not bind metal but is essential for catalysis. The reasons that the other highly conserved residues are maintained are unknown but provide a basis for future structure–function studies of these molecules. When core sequences were compared with the ALIGN program (17), with a gap penalty of 25, scores ranged from 4.8 to 19 standard deviations above a randomized score. In addition, we compared the protein cores by the pairwise comparison algorithm of Chothia and Lesk (28), which uses amino acid sequence identity to predict rms deviations in three-dimensional structures of distantly related protein families. Predicted deviations are 1.68 Å for 1-ptase vs. m-ptase, 1.90 Å for m-ptase vs. fb-ptase, and 2.06 Å for 1-ptase vs. fb-ptase, which are in agreement with the observed rms deviations. Comparison of all eight proteins in this way resulted in deviations ranging from 0.62 to 2.06 Å.

To identify additional members of this protein family, we have defined a structure-independent sequence criteria. The highly conserved Asp-Pro-(Ile or Leu)-Asp-(Gly or Ser)-(Thr or Ser) motif is not sufficient to identify family members *per se*. For example, ATPase F1 β subunit contains a Asp-Pro-Leu-Asp-Ser-Thr sequence; however inspection of its crystal structure (29) shows that it does not fit the common core structure of this family. Therefore, we expanded the sequence requirements to include other conserved metal-binding residues, as defined above, and the conserved Gly-Gly located on core element β10 (see Fig. 2*A*). Thus, by requiring these additional residues and requiring that the spacing among these residues be constrained so that the motif becomes Asp-Xaa_{22-24}-Glu-Glu-(Xaa_{15-23} or Xaa_{68-72})-Asp-Pro-(Ile or Leu)-Asp-(Gly or Ser)-(Thr or Ser)-($Xaa_{115-123}$ or $Xaa_{140-157}$)-(Trp or Tyr)-(Asp or Glu)-Xaa_{11}-Gly-Gly, we have not found any other family members in the GenBank data base. (The spacer length ranges, denoted by Xaa_{y-z}, were determined from Fig. 2*A*, and in cases where two ranges are given, the lengths conform into two distinct groups). We also evaluated this protein family using the three-dimensional profile method of Eisenberg and colleagues (30). Using the discrete profile method and published data matrix, we obtained essentially the same *Z* scores as described for several example proteins (30). We then used the coordinates of 1-ptase, fb-ptase, or m-ptase as a template and obtained *Z* scores for each sequence against its own template of 70.5, 55.4, and 62.8, respectively (using gap open, gap extension, and secondary-structure break penalties of 4.5, 0.05, and 0.0, respectively). No *Z* scores above 1.0 were obtained when either 1-ptase or fb-ptase was used as a template against other known family members under several conditions in which penalty weights were altered. However, when m-ptase was used as a template, scores of 20.0, 11.9, 8.0, 8.0, and 3.6 (using gap open, gap extension and secondary structure break penalties of 3.0, 0.06 and ∞, respectively) were obtained against SuhB, QutG, Qa-X, CysQ, and met22. Alignments of these proteins by the profile method were similar to those obtained when using TBLASTN alignments of core sequences.

While the core structures of these proteins have been maintained presumably to impart catalytic function, the loops and regions of structure outside the core have evolved unique regulatory domains. fb-ptase is allosterically regulated by AMP. The AMP binding site is formed by an additional N-terminal helix that is not present in other family members. The multimerization interfaces of m-ptase and fb-ptase are not found in 1-ptase, which exists as monomer both in crystals and in solutions. 1-ptase contains 50 additional residues (between core elements β1 and β2) that form a novel domain for which the function is not yet known. Similarly, met22 also has 45 additional residues between these elements; however, the sequence does not show any relationship to these residues of 1-ptase.

The evolutionary relationship of the core sequences of these proteins was evaluated by using the progressive alignment method of Feng and Doolittle (18) as shown in Fig. 3. It appears that these proteins diverged from a common ancestor prior to the separation of prokaryotes and eukaryotes. Five distinct branches were found corresponding to the activities of fb-ptase, 1-ptase, Qa-X/QutG (their activities are speculative at this point), m-ptase, and CysQ/met22. As this manuscript was in preparation, we learned of the activities of two previously undetermined enzymes—namely, *E. coli* SuhB and *S. cerevisiae* met22 (hal2). Matsuhisa and coworkers (31) demonstrated that SuhB is a Mg^{2+}-dependent/Li^+-inhibited phosphatase that hydrolyzes a number of phosphorylated monoesters including inositol 1-phosphate with kinetic parameters similar to those of the m-ptase enzyme. Murguia *et al.* (32) demonstrated that hal2 is a 3′(2′),5′-bisphosphate nucleotidase that utilizes 3′-phosphoadenosine 5′-phosphosulfate (PAPS), 3′-phosphoadenosine 5′-phosphate (PAP), or 2′-phosphoadenosine 5′-phosphate (2′-PAP) by removing the 3′ or 2′ phosphates. This enzyme requires Mg^{2+} and is potently inhibited by Li^+ with an IC_{50} of 0.1 mM. Interestingly, the nucleotidase activity is slightly stimulated by K^+ and slightly inhibited by Na^+, properties which have not been observed for either 1-ptase or m-ptase. CysQ, which is the most related to met22, has been implicated in the sulfate assimilation pathway of bacteria (26) and is likely the prokaryotic met22 homologue.

In addition, a mammalian 2′(3′),5′-bisphosphate nucleotidase has also been described (33) that performs the identical reaction as the yeast enzyme, suggesting that this enzyme is present from bacteria to man.

The members of this family for which structures and functions are known are all Mg^{2+}-dependent/Li^{+}-sensitive phosphomonoesterases. We predict that Qa-X/QutG proteins and other as-yet-unidentified family members for which specific substrates are not currently known will also prove to be such enzymes. Qa-X and QutG are most likely homologues to each other and are thought to function in the quinone metabolic pathway (24, 25). Thus, they most likely will have unique substrate specificity, although since Qa-X/QutG show a high degree of homology to m-ptase, it remains possible that they are its fungal counterpart.

Perhaps the most intriguing physiologic property of the enzymes in this protein family is their sensitivity to Li^{+} at levels achieved in patients undergoing therapy for manic-depressive disease. Li^{+} has been the mainstay of pharmacologic treatment of these patients since the discovery of its therapeutic efficacy >40 years ago (34). Remarkably, the targets of Li^{+}, both the therapeutic and toxic, and the mechanism of its action remains unknown. A recent theory has proposed that patients with this disorder have an "overactive" inositol phosphate signaling pathway to account for their symptoms (35). It has been suggested that inhibition of these enzymes results in "inositol depletion" in brain thereby slowing signaling reactions (36). However, definitive proof that inositol levels in human brain are "depleted" in response to therapeutic doses of Li^{+} is not likely to be obtained (37). Genetic studies of familial manic–depressive disease have failed to identify a candidate gene but have suggested that the disorder is polygenic (38). We suggest that this family of proteins represents targets for Li^{+} in manic–depressive disease, both therapeutic and toxic. Thus, by utilizing the x-ray structures of members of this family, it should be possible to design specific inhibitors of each enzyme. These inhibitors may then be used to treat patients with manic–depressive disease to validate our theory and ultimately to obtain an improved treatment for manic–depressive disease.

We thank Zhi-wei Chen and F. Scott Mathews for helpful suggestions and J. Evan Sadler for critical comments. In addition, we thank Kiyotaka Shiba for sharing data prior to its publication. This work was supported by Grants HL 14147 and HL 16634 from the National Institutes of Health and a grant from Merck Research Laboratories.

1. Inhorn, R. C. & Majerus, P. W. (1988) *J. Biol. Chem.* **263,** 14559–14565.
2. Majerus, P. W. (1992) *Annu. Rev. Biochem.* **61,** 225–250.
3. Hallcher, L. M. & Sherman, W. R. (1980) *J. Biol. Chem.* **255,** 10896–10901.
4. York, J. D. & Majerus, P. W. (1990) *Proc. Natl. Acad. Sci. USA* **87,** 9548–9552.
5. Neuwald, A. F., York, J. D. & Majerus, P. W. (1991) *FEBS Lett.* **294,** 16–18.
6. Glaser, H-U., Thomas, D., Gaxiola, R., Montrichard, F., Surdin-Kerjan, Y. & Serrano, R. (1993) *EMBO J.* **12,** 3105–3110.
7. York, J. D., Ponder, J. W., Chen, Z.-W., Matthews, F. S. & Majerus, P. W. (1994) *Biochemistry* **33,** 13164–13171.
8. Bone, R., Springer, J. P. & Atack, J. R. (1992) *Proc. Natl. Acad. Sci. USA* **89,** 10031–10035.
9. Zhang, Y., Liang, J.-Y. & Lipscomb, W. N. (1993) *Biochem. Biophys. Res. Commun.* **190,** 1080–1083.
10. Gomori, G. (1943) *J. Biol. Chem.* **148,** 139–149.
11. Mokrasch, L. C. & McGilvery, R. W. (1956) *J. Biol. Chem.* **221,** 909–917.
12. Nakashima, K. & Tuboi, S. (1976) *J. Biol. Chem.* **251,** 4315–4321.
13. Marcus, F. & Hosey, M. M. (1980) *J. Biol. Chem.* **255,** 2481–2486.
14. Benkovic, S. J. & DeMoine, M. M. (1982) *Adv. Enzymol.* **53,** 45–82.
15. Ke, H., Thrope, C. M., Seaton, B. A., Marcus, F. & Lipscomb, W. N. (1989) *Proc. Natl. Acad. Sci. USA* **86,** 1445–1449.
16. Altschul, S. F., Gish, W., Miller, W., Myers, E. W. & Lipman, D. J. (1990) *J. Mol. Biol.* **215,** 403–410.
17. Dayhoff, M. O., Barker, W. C. & Hunt, L. T. (1983) *Methods Enzymol.* **91,** 524–545.
18. Devereux, J., Haeberli, P. & Smithies, D. (1984) *Nucleic Acids Res.* **12,** 387–395.
19. Feng, D. F. & Doolittle, R. F. (1987) *J. Mol. Evol.* **25,** 351–360.
20. Pollack, S. J., Knowles, M. R., Atack, J. R., Broughton, H. B., Ragan, C. I., Osborne, S. A. & McAllister, G. (1993) *Eur. J. Biochem.* **217,** 281–287.
21. York, J. D. (1993) Ph.D. thesis (Washington University, St. Louis).
22. Bone, R., Frank, L., Springer, J. P., Pollack, S. J., Osborne, S., Atack, J. R., Knowles, M. R., Mcallister, G., Ragan, C. I., Broughton, H. B., Baker, R. & Fletcher, S. R. (1994) *Biochemistry* **33,** 9460–9467.
23. Petsko, G. A., Kenyon, G. L., Gerlt, J. A., Ringe, D. & Kozarich, J. W. (1993) *Trends Biol. Sci.* **18,** 372–376.
24. Hawkins, A. R., Lamb, H. K., Smith, M., Keyte, J. W. & Roberts, C. F. (1988) *Mol. Gen. Genet.* **214,** 224–231.
25. Asch, D. K., Orejas, M., Geever, R. F. & Case, M. E. (1991) *Mol. Gen. Genet.* **230,** 337–344.
26. Thomas, D., Barbey, R. & Surdin-Kerjan, Y. (1990) *J. Biol. Chem.* **265,** 15518–15524.
27. Neuwald, A. F., Krishnan, B. R., Brikun, I., Kulakauskas, S., Suzieldelis, K., Tomcsanyi, T., Leyh, T. S. & Berg, D. E. (1992) *J. Bacteriol.* **174,** 415–425.
28. Chothia, C. & Lesk, A. M. (1986) *EMBO J.* **5,** 823–826.
29. Abrahams, J. P., Leslie, A. G. W., Lutter, R. & Walker, J. E. (1994) *Nature (London)* **370,** 621–628.
30. Bowie, J. U., Luthy, R. & Eisenberg, D. (1991) *Science* **253,** 164–170.
31. Matsuhisa, A., Suzuki, N., Noda, T. & Shiba, D. (1995) *J. Bacteriol.* **177,** 200–205.
32. Murguia, J. R., Belles, J. M. & Serrano, R. (1995) *Science* **267,** 232–234.
33. Ramaswamy, S. G. & Jakoby, W. B. (1987) *J. Biol. Chem.* **262,** 10033–10047.
34. Cade, J. F. (1949) *Med. J. Aust.* **36,** 349–352.
35. Berridge, M. J., Downes, C. P. & Hanley, M. R. (1989) *Cell* **49,** 411–419.
36. Allison, H. J. & Stewart, M. A. (1971) *Nature (London) New Biol.* **233,** 267–268.
37. Baraban, J. M. (1994) *Proc. Natl. Acad. Sci. USA* **91,** 5738–5739.
38. Hodgkinson, S., Sherrington, R., Gurling, H., Marchbanks, R., Reeders, S., Mallet, J., McInnis, M., Petursson, H. & Brynjolfsson, J. (1987) *Nature (London)* **325,** 805–806.